

**FINITE ELEMENT ANALYSIS OF THE BONDCOAT INFLUENCE
ON RESIDUAL STRESS DURING THE PLASMA THERMAL SPRAYING
OF PARTIALLY STABILISED ZIRCONIA**

P. Fogarassy^(1,2), F. Rotaru⁽¹⁾, N. Markocsan⁽¹⁾, B.B. Straumal⁽³⁾
(1) Institutul Național de C&D în Sudare și Încercări de Materiale
(ISIM) Timișoara, ROMANIA,
(2) Universitatea “Politehnica” Timișoara, ROMANIA
(3) I.V.T. Ltd. (Institute for Vacuum Technology) Moscow, RUSSIA

1. Formation of stresses during the plasma spray process

The formation of stresses in plasma sprayed coatings can be divided in three stages [4]. The first stage concerns solidification of single particles. Due to the great temperature difference between the substrate and the particles, tensile stress will occur in these particles. In literature, this first stage is called primary cooling.

The second stage involves the heating up of the substrate during the coating process, caused by the heat transport from the coating to the substrate. This results in expansion of the substrate causing tensile stress in the already deposited part of the coating. Next to this, the newly deposited layers solidify on a dilated substrate.

The third stage concerns the stresses caused by the cooling down of the substrate and the coating together after the coating process has been completed. In literature this third stage is known as secondary cooling. These three stages together determine the ultimate residual stress in the coating and the substrate.

In literature [4], strains due to primary cooling are mainly represented by the equation (1.1).

$$\varepsilon = \alpha_c (T_m - T_s) \quad (1.1)$$

where: ε – strain in the particle;
 α_c – coefficient of thermal expansion of particle [K^{-1}];
 T_m – melting point of the particle [K];
 T_s – substrate temperature [K].

The contact temperature between ceramic and the metallic substrate materials are relatively low. This indicates that the temperature on the solidifying particle, near the substrate is also low. Therefore, this part of the coating can not be deformed plastically during shrinking. When a certain strain is exceeded, crack formation occurs, resulting in the dense crack network in the single ceramic particle.

After solidification, the temperature in the particle rapidly drops to the substrate temperature T_s . [3] The substrate below the solidified particle expands due to the latent heat of the particle. The maximum strain caused by cooling down from the contact temperature to the substrate temperature according to equation (1.2).

$$\varepsilon_{T_c-T_s} = (\alpha_c - \alpha_s) \cdot (T_c - T_s) \quad (1.2)$$

where: α_s – substrate coefficient of thermal expansion [K^{-1}];

T_s – substrate temperature [K].

The strain in a particle at room temperature is equal to the tensile strain caused by cooling down from T_m to T_c minus the strain caused by the shrinking metallic substrate. When the substrate and coating material are the same, the strain will depend only on the contact temperature.

The stresses caused by heating up and cooling down of the substrate during the spraying process produce compressive stress in the deposited coatings because these were solidified on a dilated substrate and the substrate shrinks more than the ceramic coating.

The finite element analysis presented in this paper will evaluate the value and the distribution of the stress due to the secondary cooling. The stresses introduced in the ceramic layer due to the primary cooling are neglected in this model.

2. Residual stress measurement and evaluation

Prediction and understanding of the residual stresses that develop during the thermal spraying process is an important goal in order to improve the quality of thermal deposited layers. The stress distribution in the substrate and deposited coatings determine various characteristics of this, such as its resistance to spallation in different conditions.

Different techniques are used to directly measure the residual stress level in sprayed coatings. One of the most used methods is monitoring of the shift of selected X-ray diffraction peaks. However, results published in different papers are not always reliable. The reason for this affirmation is that the x-ray penetration is about 10-50 μm , which is usually less than surface roughness of the sprayed coatings. Therefore the measured strains are only evaluated in a region where significant stress relaxation occurs. Another source of errors arises from variation of stresses with depth. The removals of layers change the stress distribution, not only because of the mechanical process, but also because of the missing effect of the removed layers [1].

There exists certain alternative techniques for investigation of residual stresses, such as neutron diffraction and hole drilling. However, these techniques are sometime inadequate or unavailable for the study of residual stresses in sprayed coatings.

Finite Element Analysis method was used in this paper in order to estimate the stress distribution in plasma thermal sprayed coatings and substrate. The validation of the calculated results will be performed in a future experimental program.

3. Modelling condition

In this study, a zirconia (ZrO_2) layer partially stabilised with yttria (Y_2O_3) was sprayed on AISI 316 steel. The aim of this study is to determine the influence of a NiCrAlY interlayer upon the stress distribution in the ceramic layer.

In the figure 3.1 is presented the geometry of the samples.

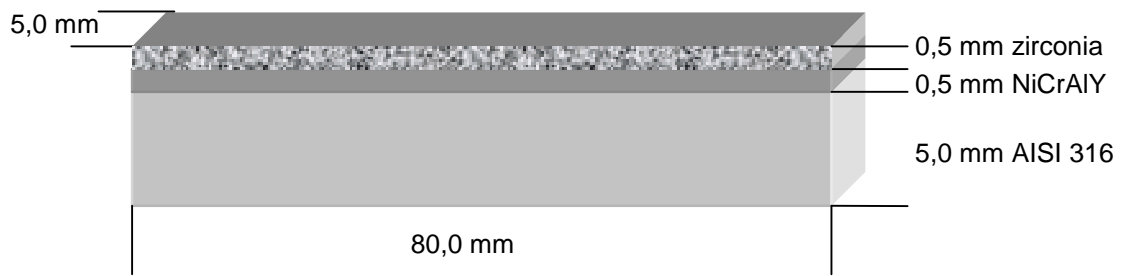


Figure 3.1 The geometry of the analysed samples

In the table 3.1 are presented the physical properties of materials.

Table 3.1 Physical properties of materials

| Material | Thermal conductivity λ [$\text{W}\cdot\text{m}^{-1}\cdot\text{K}^{-1}$] | Density ρ [$\text{kg}\cdot\text{m}^{-3}$] | Specific heat C [$\text{J}\cdot\text{kg}^{-1}\cdot\text{K}^{-1}$] | Melting temperature T_m [C] | Young modulus E [$\text{N}\cdot\text{m}^{-2}$] | Poisson Coeff. ν | Expansion coeff. α [K^{-1}] |
|---|--|---|--|----------------------------------|---|-------------------------|--|
| NiCrAlY | 10.0 | 8050 | 450 | 1350 | $195\cdot 10^9$ | 0.31 | $14\cdot 10^{-6}$ |
| ZrO ₂ + 8% Y ₂ O ₃ | 1.5 | 5000 | 477 | 2670 | $40\cdot 10^9$ | 0.22 | $10\cdot 10^{-6}$ |
| AISI 316 | 18.0 | 7670 | 489 | 1375 | $200\cdot 10^9$ | 0.27 | $16\cdot 10^{-6}$ |

As one can see, there exist differences between the expansion coefficients of the involved materials; therefore, residual stresses are expected when the heated structures are cooled down, after the thermal spraying process.

It is assumed a uniform 800 K cooling process for all the materials together and during the cooling, it is assumed also a uniform spatial temperature distribution.

4. Finite element analysis

4.1 Meshing

In the figure 4.1 it is presented the finite element mesh. The mesh density is a compromise between the need of accuracy (finer mesh in the areas with higher gradients) and the need for faster analysis (small number of degrees of freedom, therefore small number of nodes).

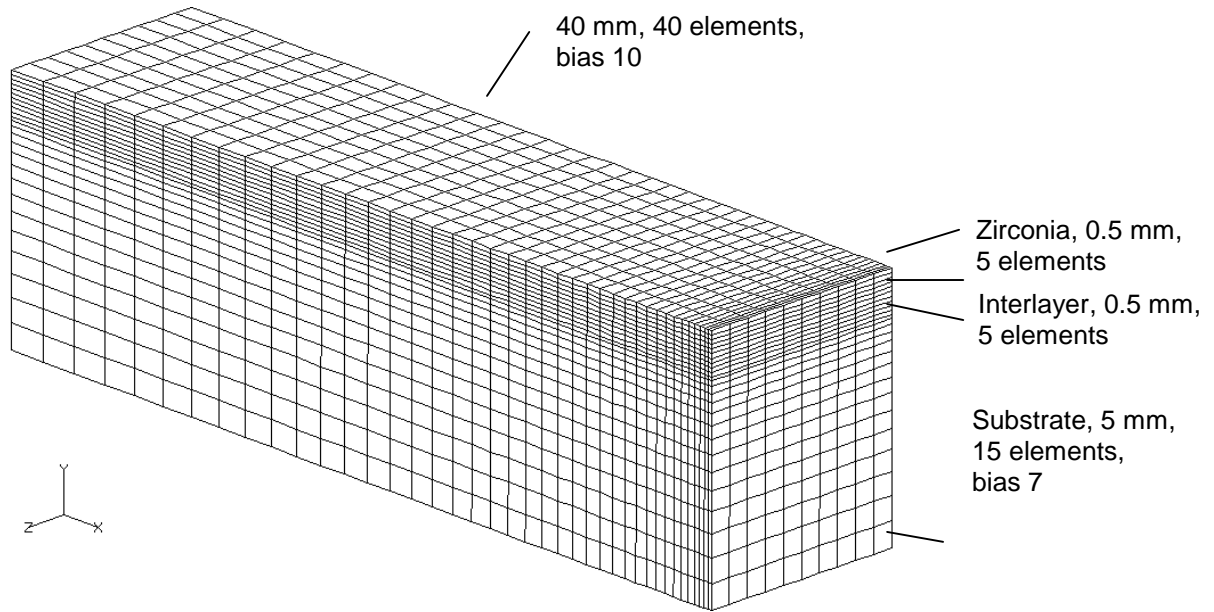


Figure 4.1 The finite element mesh

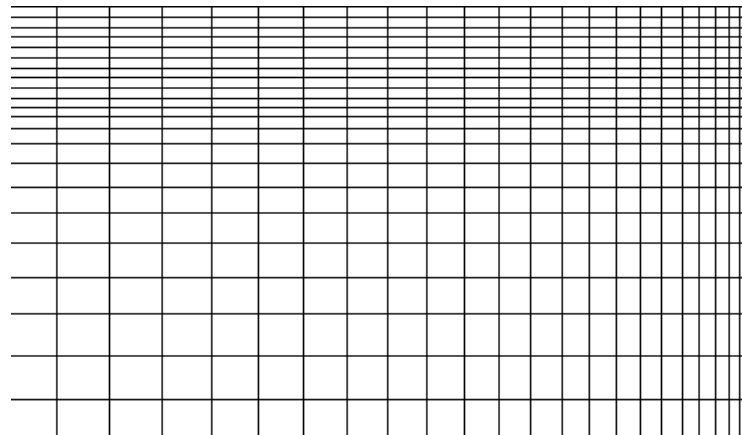


Figure 4.2 Progressive mesh refinements on two directions (details)

In order to meet this compromise the mesh density is progressively finer from low to higher stress gradients, both on X and Y directions, as can be seen in the figure 4.1.

Another advantage of progressive mesh refinement (see figure 4.2 for details), is the avoiding of numerical problems occurring in the areas where small and big elements are meeting.

4.2 Deformations

In figure 4.3 it is presented the tri-dimensional deformation of the sample (half), after the cooling down from the plasma spraying temperature with 800 K.

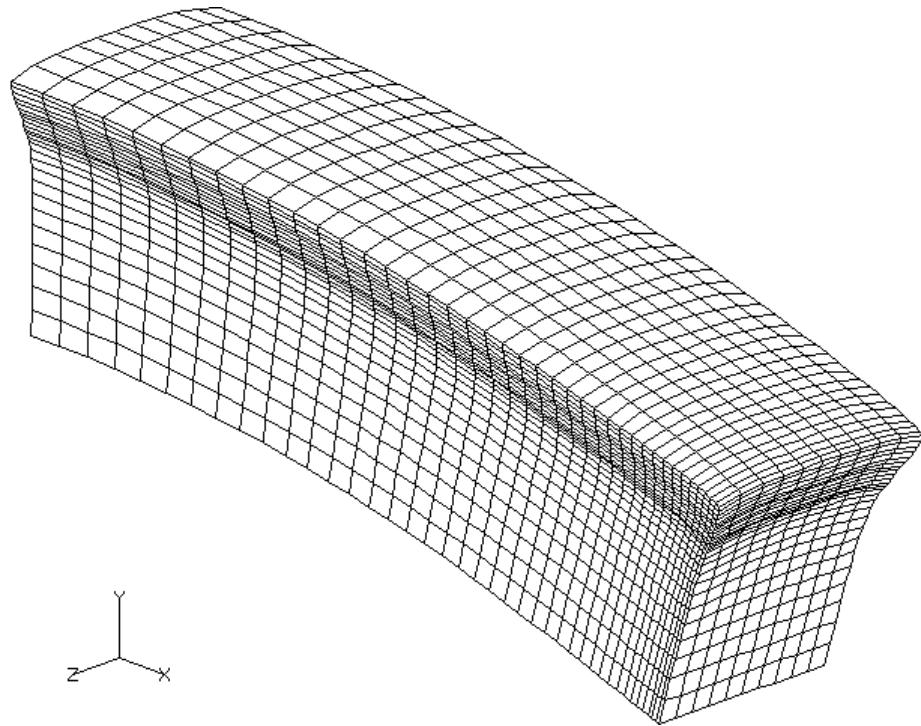


Figure 4.3 Tri-dimensional deformation of the sample (half)

As one can see, because of smaller thermal expansion coefficient (see table 3.1) the coating materials are compressed by the deformation of the substrate.

In figure 4.4 a detail of the distorted structure can be observed. Even the difference between the coating material and interlayer material deformation can be distinguished in this detail.

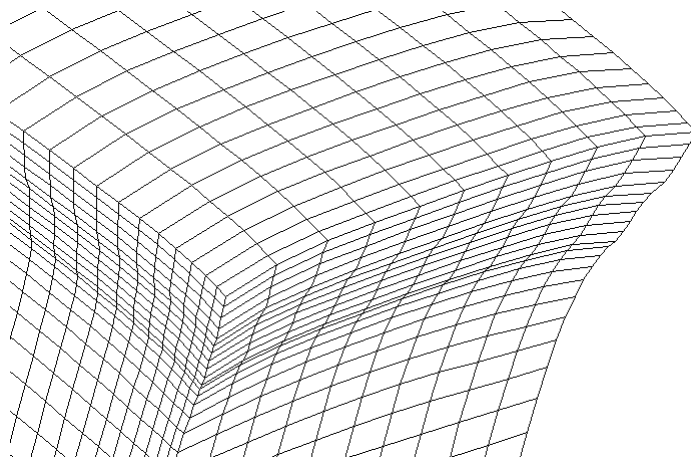
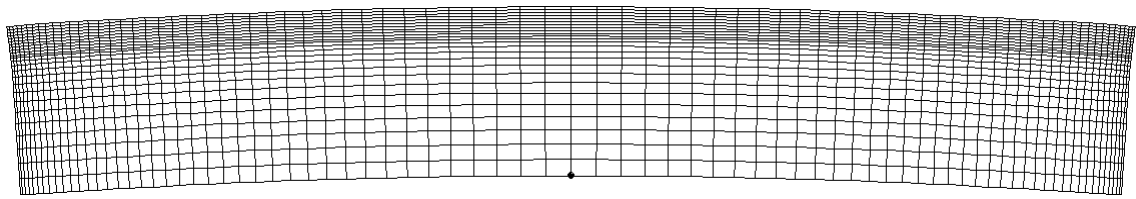
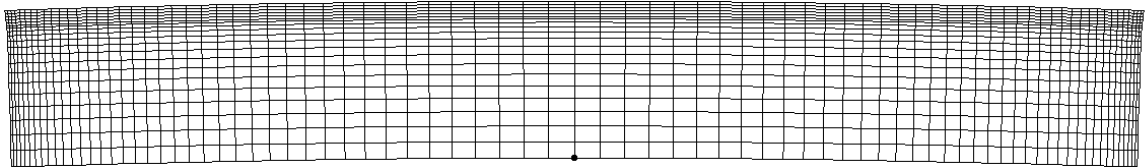


Figure 4.4 Detail of the distorted structure

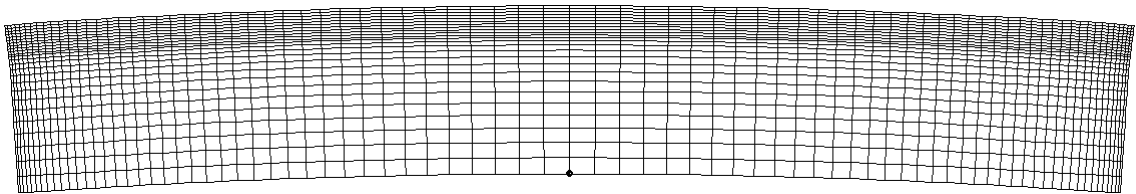
In the figure 4.5 are presented the distorted structures, for different type of coating. As one can see, there are (as we expect) significant differences, from this point of view.



a) NiCrAlY and $ZrO_2+8\% Y_2O_3$



b) NiCrAlY



c) $ZrO_2+8\% Y_2O_3$

Figure 4.5 The distorted structures, for different type of coating

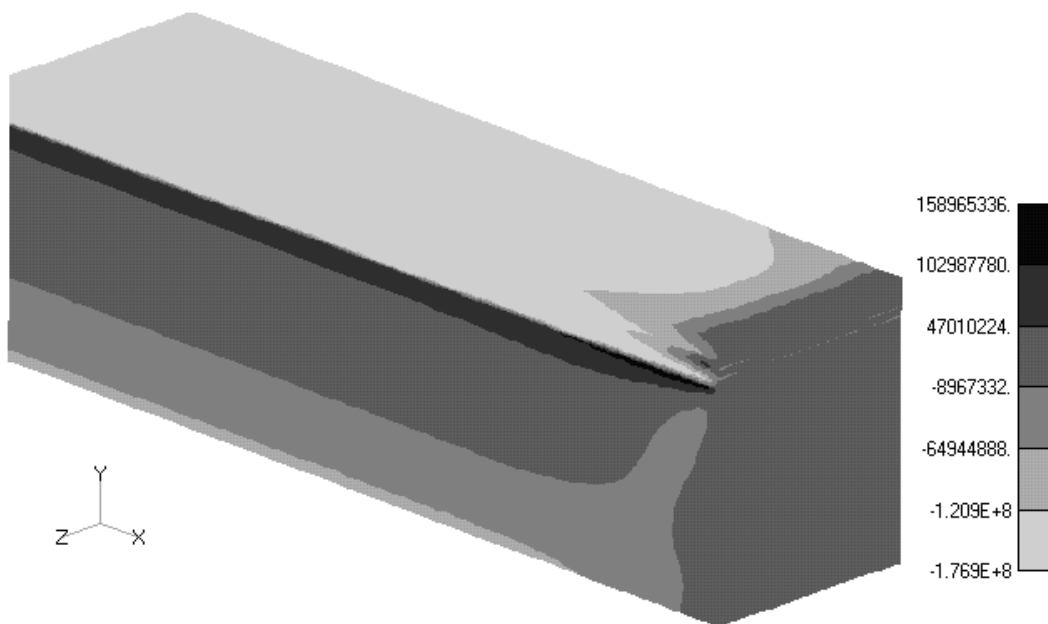
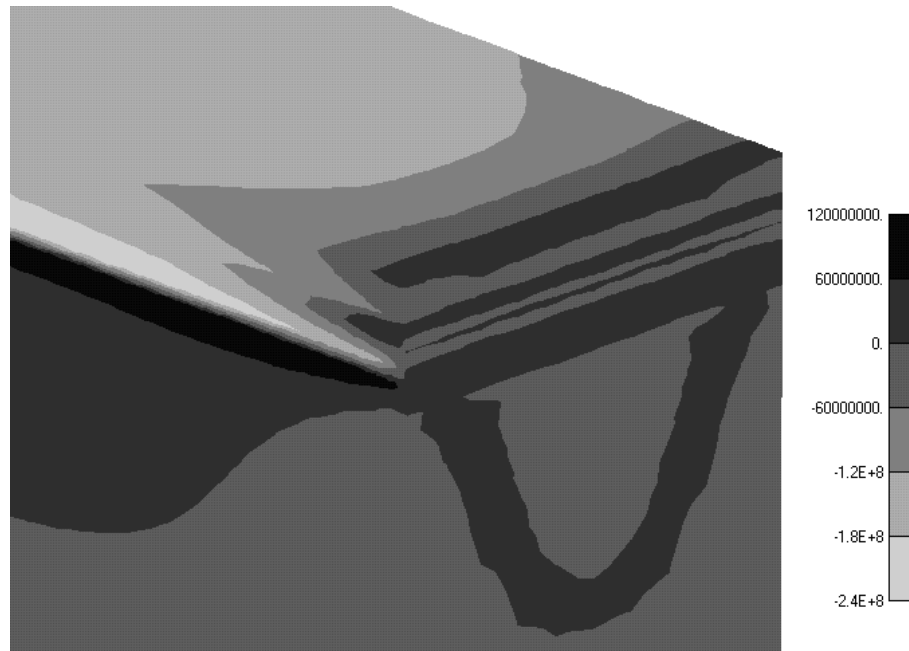


Figure 4.6 The normal X stress distribution [Pa]

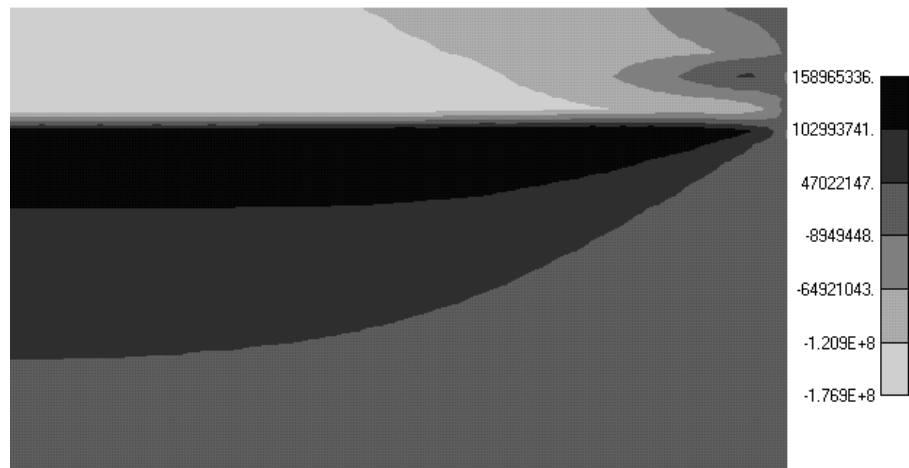
4.3 Stresses distribution

Figure 4.6 show the normal X stress distribution for the substrate, interlayer and the bondcoat. As we expect, stress concentrations appear at the edge of the sample. This is called the edge effect and lead to spallation of the coated layer in this area, more often then in other areas.

Figure 4.7 present a detail of the normal X stress distribution. As one can see, the topcoat (ceramic layer) is subject to lower compressive stress then the interlayer (NiCrAlY). From this point of view, the interlayer has the role of stress relaxation for the ceramic material.



a) 3D presentation



b) 2D presentation

Figure 4.7 Detail of the normal X stress distribution [Pa]

On the other hand, in the figure 4.8 the equivalent Von Mises stress distribution is presented.

As can be observed, the first stress concentration is located at the interface between the substrate and interlayer and another stress concentration is located at the interface between the topcoat and interlayer.

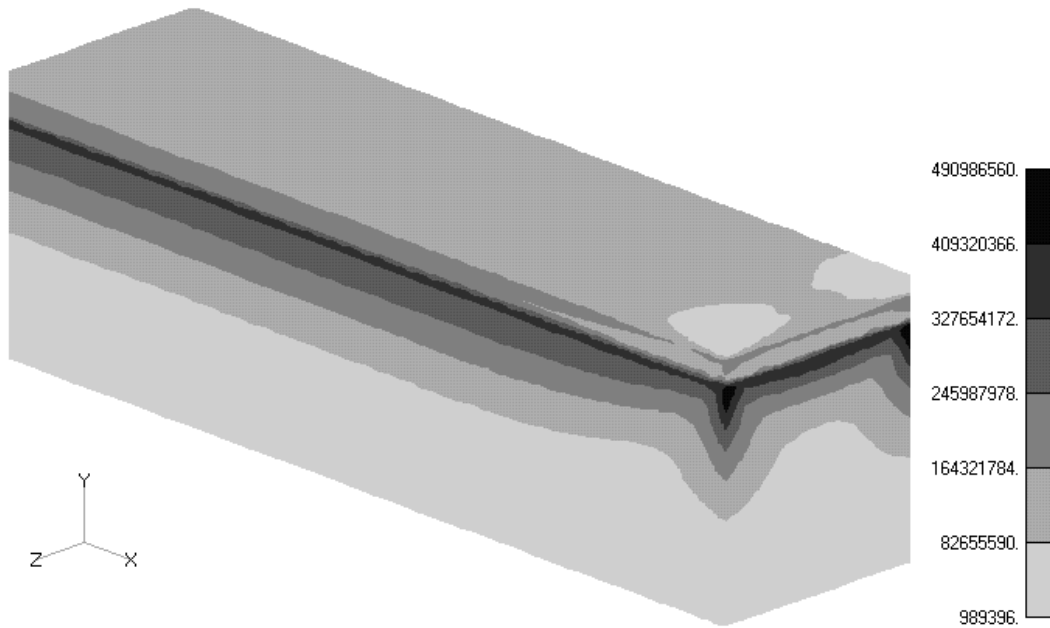
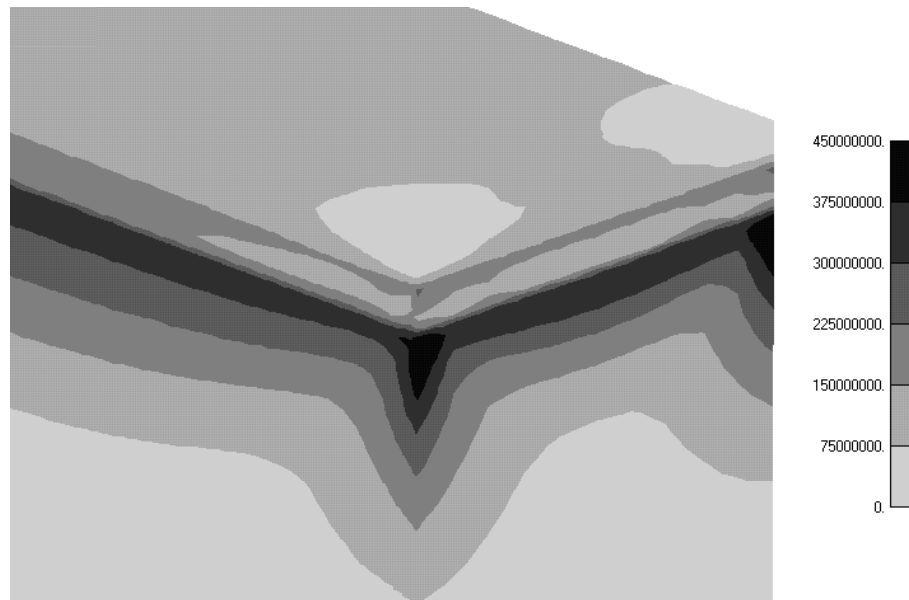
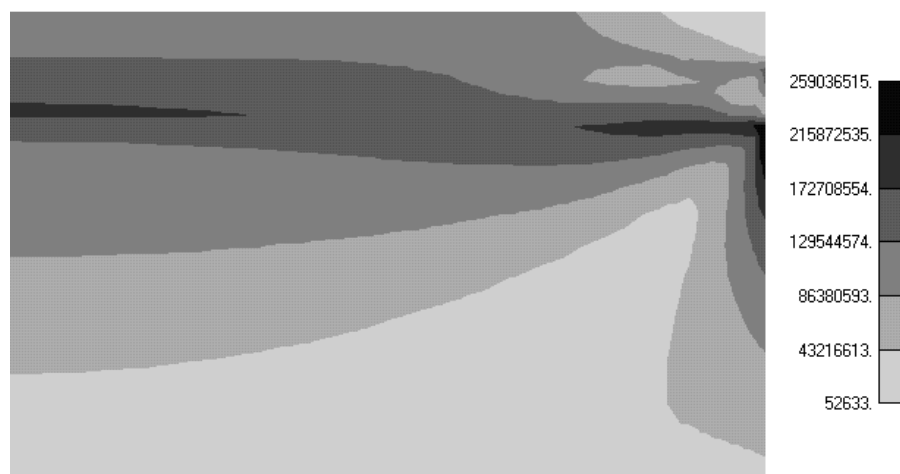


Figure 4.8 Equivalent Von Mises stress distribution [Pa]

The detail presented in figure 4.9 reveal the distribution of the above mentioned edge effect. The important effect of stress relaxation of the interlayer upon the ceramic layer can be observed.



a) 3D presentation



b) 2D presentation

Figure 4.9 Detail of the edge effect (Von Mises stress) [Pa]

The high concentration of stress on the edge of the component is strongly related to shear stress concentration in this area. The figure 4.10 presents a detail of the shear stress in the XZ direction.

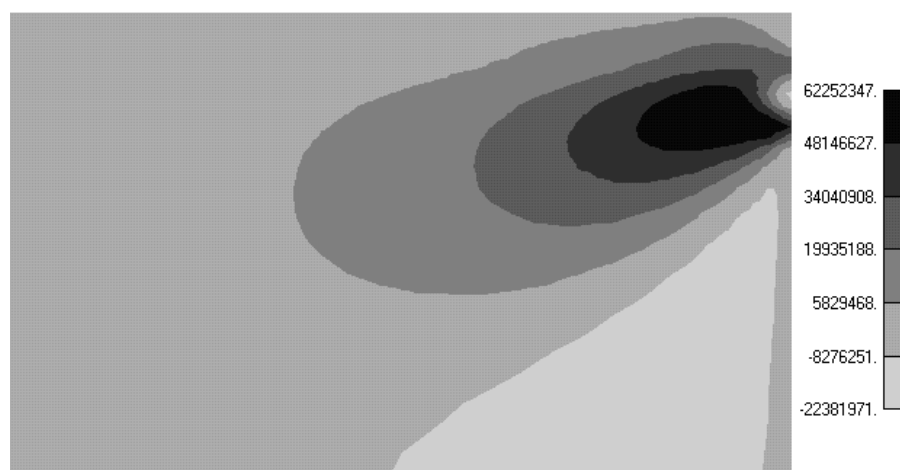


Figure 4.10 Detail of shear stress concentration on the edge of the component [Pa]

5. Conclusions

The stresses produced by secondary cooling could be calculated from the Hooke's law, assuming the infinite plate hypothesis. Unfortunately this approximation is not useful for the edge effect calculation.

Without the presence of a NiCrAlY interlayer, the compressive stress in the ceramic layer is higher and the danger of spallation increase during the cooling down of the structure. Moreover, the bondcoat have also the effect of stress relaxation.

Finite element analysis is an excellent tool in decision about the geometry and dimension of the deposited layers and bondcoat material selection.

References

- [1] Gill, S.C., Clyne, T.W., Monitoring of Residual Stress Generation During Thermal Spraying by Curvature Measurements, Proceedings of the 7th National Spray conference, 1994, Boston Massachusetts
- [2] Bartlett, A.H., Castro, R.G., Residual stress in Net-Shape Plasma Sprayed Tubes: Measurement, Modelling and Modification, Thermal Spray: Practical Solutions for Engineering Problems, ASM International, Materials Park, Ohio-USA, 1996
- [3] Pejyrd, L., Wigren, J., Residual Stress Development during Thermal Spraying of WC-Co on Titanium, Thermal Spray: Practical Solutions for Engineering Problems, ASM International, Materials Park, Ohio-USA, 1996
- [4] Verbeek, A.T.J., – Plasma Sprayed Thermal Barrier Coatings. Production, Characterisation and Testing, Eindhoven University, 1993